Development 137, 1689-1698 (2010) doi:10.1242/dev.047464

Biogenesis of GPI-anchored proteins is essential for surface expression of sodium channels in zebrafish Rohon-Beard neurons to respond to mechanosensory stimulation

Yuri Nakano[1], Morihisa Fujita[2,3], Kazutoyo Ogino[1], Louis Saint-Amant[4], Taroh Kinoshita[2,3,5], Yoichi Oda[1] and Hiromi Hirata[1,*]

SUMMARY

In zebrafish, Rohon-Beard (RB) neurons are primary sensory neurons present during the embryonic and early larval stages. At 2 days post-fertilization (dpf), wild-type zebrafish embryos respond to mechanosensory stimulation and swim away from the stimuli, whereas *mi310* mutants are insensitive to touch. During ~2-4 dpf, wild-type RB neurons undergo programmed cell death, which is caused by sodium current-mediated electrical activity, whereas mutant RB cells survive past 4 dpf, suggesting a defect of sodium currents in the mutants. Indeed, electrophysiological recordings demonstrated the generation of action potentials in wild-type RB neurons, whereas mutant RB cells failed to fire owing to the reduction of voltage-gated sodium currents. Labeling of dissociated RB neurons with an antibody against voltage-gated sodium channels revealed that sodium channels are expressed at the cell surface in wild-type, but not mutant, RB neurons. Finally, in *mi310* mutants, we identified a mis-sense mutation in *pigu*, a subunit of GPI (glycosylphosphatidylinositol) transamidase, which is essential for membrane anchoring of GPI-anchored proteins. Taken together, biogenesis of GPI-anchored proteins is necessary for cell surface expression of sodium channels and thus for firings of RB neurons, which enable zebrafish embryos to respond to mechanosensory stimulation.

KEY WORDS: Zebrafish, Sodium channel, Behavior, Rohon-Beard neuron, GPI-anchored protein, GPI transamidase, Touch response

INTRODUCTION

Rohon-Beard (RB) neurons are primary sensory neurons in the embryonic spinal cord in lower vertebrates such as lamprey, teleosts and amphibians (Roberts, 2000). They are located bilaterally in the dorsal spinal cord. A RB neuron has a cell body, two central axons and a peripheral axon. One central axon projects rostrally to the hindbrain and another caudally within the spinal cord, whereas the peripheral axon extends dorsolaterally from the spinal cord, runs through segmental myotomes and innervates skin, where free nerve endings are formed (Bernhardt et al., 1990; Metcalfe et al., 1990). The cell body of a RB neuron (~15-20 μm diameter) is significantly larger than those of the other spinal neurons (~10 μm diameter). The zebrafish RB neurons exhibit caspase-dependent programmed cell death during normal development and their function is replaced by dorsal root ganglia neurons (Williams et al., 2000; Cole and Ross, 2001; Reyes et al., 2004). Although the mechanism to induce the apoptosis is unknown, antibodies that block neurotrophin 3 (NT3) function increase the number of dying RB cells and, on the contrary, application of exogenous NT3 diminishes the extent of RB cell death (Williams et al., 2000). siRNA-mediated knockdown of cyclin-dependent kinase 5 (Cdk5) promotes the programmed cell death of RB neurons, whereas overexpression of Cdk5 decreases the RB cell death (Kanungo et al., 2006). Interestingly, a reduction in sodium currents either by an inhibitor of voltage-gated sodium channels or by antisense-mediated knockdown of an α subunit of voltage-gated sodium channels (Nav1.6a) also decreases the RB cell death (Svoboda et al., 2001; Pineda et al., 2006), thereby suggesting that neurotrophic inputs, kinase regulations and electrical activity provide signals that are required for the normal elimination of RB neurons.

The large-scale Tübingen mutagenesis screen isolated 63 zebrafish mutants that showed abnormal touch responses (Granato et al., 1996). Among them, six mutants, including *macho*, *alligator* and *steifftier*, were less sensitive to tactile stimuli than wild-type embryos. Electrophysiological analyses revealed that the RB neurons in these mutants do not generate action potentials, owing to a reduction of voltage-gated sodium currents (Ribera and Nüsslein-Volhard, 1998). The programmed cell death of RB neurons was significantly decreased in *macho* mutants, corroborating the notion that *macho* mutants have defects in RB neurons (Svoboda et al., 2001). However, the responsible genes of either *macho* or other *macho*-class mutants have not yet identified.

In this paper, we characterized a novel touch-insensitive mutant, *mi310*. Similar to in the *macho* mutant, cell death of RB neurons was decreased in *mi310*. Patch-clamp recording revealed that action potentials were impaired in mutant RB cells. Immunostaining disclosed that cell surface distribution of sodium channels was deceased in mutant RB neurons. In *mi310*, the *pigu* gene, which

[1]Graduate School of Science, Nagoya University, Nagoya 464-8602, Japan. [2]Department of Immunoregulation, Research Institute for Microbial Disease, Osaka University, Suita 565-0871, Japan. [3]Core Research for Evolutional Science and Technology, Japan Science and Technology Agency, Saitama 332-0012, Japan. [4]Département de Pathologie et Biologie Cellulaire, Université de Montréal, Montréal, QC H3T 1J4, Canada. [5]Laboratory of Immunoglycobiology, WPI Immunology Frontier Research Center, Osaka University, Suita 565-0871, Japan.

*Author for correspondence (hhirata@bio.nagoya-u.ac.jp)

Accepted 11 March 2010

encodes for a subunit of glycosylphosphatidylinositol (GPI) transamidase, carried a mis-sense mutation that abolishes enzyme activity. GPI transamidase transfers GPI to proteins bearing the GPI attachment signal sequence, thereby forming GPI-anchored proteins (Kinoshita et al., 2008). Therefore, biogenesis of GPI-anchored proteins is necessary for proper cell surface expression of sodium channels to generate action potentials in RB neurons that enable embryos to respond to tactile stimulation.

MATERIALS AND METHODS

Animals

Zebrafish were bred and raised according to the established protocols (Nüsslein-Volhard and Dahm, 2002; Westerfield, 2007), which meet the guidelines set forth by Nagoya University. The *mi310* mutation was isolated in an *N*-ethyl-*N*-nitrosourea mutagenesis performed at the University of Michigan (Hirata et al., 2004). The zCREST2-hsp70:GFP transgenic line was provided from Dr H. Okamoto (RIKEN) (Uemura et al., 2005). The Zebrafish hb9:Venus transgenic line was generated by Tol2-mediated genomic integration (Kawakami et al., 2000) of an expression construct, which drives Venus (a bright variant of GFP) (Nagai et al., 2002) expression in motoneurons by the zebrafish hb9 promoter (–3132 to approximate start of translation) (Flanagan-Steet et al., 2005) with a polyadenylation signal of SV40.

Video recording of zebrafish behavior

Embryonic behaviors were observed and video recorded at 48 hours post-fertilization (hpf) using a dissection microscope (Leica, MZ16). Touch responses elicited by mechanosensory stimulation delivered to the tail with an eyelash were captured with a high-speed CCD camera at 500 frames per second (fps) (Fastcam-Ultima1024, Photron). Spontaneous swimming in the absence and presence of 100 μM NMDA in bath solution was captured by a general-purpose movie camera at 30 fps (Xacti DMX-HD2, Sanyo).

Electrophysiology

The dissection protocols for in vivo patch recordings in RB neurons have been described elsewhere (Ribera and Nüsslein-Volhard, 1998; Pineda et al., 2005). We used zebrafish embryos [2 days post-fertilization (dpf)] carrying the zCREST2-hsp70:GFP transgene (Uemura et al., 2005).

Mapping

mi310 carrier fish were crossed with WIK (Wild-type Kalkutta) fish to generate mapping carriers that were crossed to identify mutants for the meiotic mapping to microsatellites (Gates et al., 1999; Shimoda et al., 1999) as described previously (Bahary et al., 2004). The following PCR primers were designed to narrow down the responsible region: BX530017#2 forward, 5′-GACATTGCAACTGGAACACG-3′; BX530017#2 reverse, 5′-CAACTTGCCTGCTTTTCTCA-3′; BX530017#7 forward, 5′-CAGGACCGAGTTTGGACACC-3′; BX530017#7 reverse, 5′-GACAACACCACAGACAGTGAACATG-3′; CT030737#10 forward, 5′-CCATGTAATTATACAGATTATCCTTTTAAACCAC-3′; and CT030737#10 reverse, 5′-GATGAAGGTGGTGCTGGAGTG-3′.

Cloning, mRNA rescue and antisense knockdown

The following primers were used for cloning of zebrafish *pigu* cDNA: forward, 5′-CTTCTTCCTCGCGACAAAAATGGCG-3′ and reverse, 5′-GAGCTCTCAGTCCAGTGAAAGAAGG-3′. For mRNA rescue, the coding sequence of wild-type and mutant *pigu* cDNA were subcloned in pBS bovine growth hormone (BGH), which contains an additional polyadenine signal of BGH under the T7 promoter (Hirata et al., 2005). In vitro transcription was performed with the mMESSAGE mMACHINE T7 Kit (Ambion). One hundred nanograms of capped wild-type or mutant *pigu* mRNA was injected into 1- to 4-cell stage embryos of *mi310* heterozygous incross and examined the touch response at 2 dpf. For genotyping, genomic DNA were extracted from individual mRNA-injected embryos (n=95) and subjected to genomic PCR. The 95 embryos were classified into 22 homozygous wild-type (+/+), 42 heterozygous (+/m) and 31 mutant homozygous (m/m) embryos. The following primers were used for genomic PCR and sequence reaction: genotyping forward primer, 5′-GCAGAATCGCTGATATCGTGATATATCAATACCGC-3′; genotyping reverse primer, 5′-CCAAACAGTCAGCAGGATACCG-3′; and genotyping sequence primer, 5′-GTCTCATTGCATAGCCCTGGTG-3′.

Antisense knockdown was done as described previously (Nasevicius and Ekker, 2000). The CAT sequence in bold corresponds to the start ATG codon. The sequence of antisense morpholinos (MOs) are as follows: *pigu* antisense MO, 5′-AGTGTTAAAGGAGCCGC**CAT**TTTTG-3′; *gpi8* antisense MO, 5′-AAATTGGAATAATC**CAT**TATCGTTC-3′; control MO, 5′-CCTCTTACCTCAGTTACAATTTATA-3′; *contactin1a* MO, 5′-AAGGCCTCTGGAATCATGGCTTAC-3′; *contactin2* MO, 5′-CCA-CACCCAGACCAGACACTTATTT-3′; *contactin4a* MO, 5′-AGTTTC-CATAGCAACTTCATCTTC-3′; *contactin4b* MO, 5′-AGCAGTTTC-CATGACAACCCCATTT-3′; *contactin5* MO: 5′-AGGACGAACT-GTCTGCCTTCATCC-3′.

Complementation test in Pigu-deficient CHO cells

The coding sequences of wild-type and mutant zebrafish Pigu were subcloned in pME 3HSV expression vector (Hong et al., 2003) to generate zPigu-3HSV and zPigu(I86R)-3HSV fusion proteins, respectively. The corresponding I86R mutation was introduced into the hPIGU-3HSV construct to generate hPIGU(I86R)-3HSV. We separately electroporated both of these constructs and the control vector into Pigu-deficient CHO cells (CHOPA16.1; Hong et al., 2003). Cells were labeled with anti-CD59 (5H8) or anti-DAF (IA10, Becton Dickinson) followed by PE-conjugated goat anti-mouse IgG (Becton Dickinson), and subjected to flow cytometry using a FACSCalibur (Becton Dickinson).

Immunoblot

Whole cell extracts were prepared from the aforementioned electroporated CHO cells. 50 μg of protein was separated by 10% sodium dodecyl sulfate-polyacrylamide gel electrophoresis (SDS-PAGE) and immunoblotted onto polyvinylidene difluoride membrane. Anti-HSV (mouse IgG_1, 1/2000, Novagen) and anti-calnexin (SPA-860, rabbit polyclonal, 1/1000, Stressgen) were used as primary antibodies.

In situ hybridization

The antisense and sense strands of zebrafish *pigu* probes covering the whole coding sequence were used for wholemount in situ hybridization as described previously (Hirata et al., 2007). Signal was visualized by anti-digoxigenin Fab fragments conjugated to alkaline phosphatase (Roche) with the color substrate Nitroblue Tetrazolium/5-bromo-4-chloro-3-indolyl phosphate (NBT/BCIP, Roche).

Immunostaining and TUNEL labeling

Zebrafish embryos were anaesthetized in 0.02% tricaine and pinned on a silicone dish with tungsten wires (30 μm diameter). After peeling off the skin at the trunk region, embryos were fixed in 4% paraformaldehyde at room temperature for 1 hour and then subjected to immunostaining as described previously (Hirata et al., 2007). The following primary antibodies were used during this step: anti-pan Nav (SP19, rabbit polyclonal, 1/500, Sigma); anti-HuC/D (16A11, mouse IgG_{2b}, 4 μg/ml, Invitrogen); anti-acetylated-α-tubulin (6-11B-1, mouse IgG_{2b}, 1/2000, Sigma); 3A10 [mouse IgG_1, 1/50, Developmental Studies Hybridoma Bank (DSHB)]; znp-1 (mouse IgG, 1/50, DSHB); SV2 (anti-synaptophysin, mouse IgG_1, 1/50, DSHB); F59 (anti-myosin, mouse IgG_1, 1/50, DSHB); and MF20 (anti-myosin, mouse IgG_{2b}, 1/20, DSHB). Alexa 488-conjugated anti-rabbit IgG and Alexa 568-conjugated anti-mouse IgG were used as secondary antibodies (1/1000, Invitrogen). Fluorescent images were captured by confocal microscopy (FV500, Olympus). For double labeling with anti-HuC and TUNEL, the ApopTag Fluorescein In Situ Apoptosis Detection Kit (Chemicon) was used to label dying cells as described elsewhere (Sidi et al., 2008).

Immunocytochemistry of dissociated RB neurons

Dissociation of RB neurons has been described elsewhere (Andersen et al., 2002). Cells were fixed in 4% paraformaldehyde at room temperature for 1 hour, washed with PBS and incubated with blocking buffer (1% BSA and 5% heat-inactivated goat serum in PBS) for 1 hour. Cells were incubated with anti-zScn1bb [rabbit polyclonal, 1/500, gift from L. Isom (University of Michigan)] in blocking buffer with or without 0.5% Triton X-100 (TX-100) for 1 hour and then reacted with anti-GFP (3E6, mouse IgG_{2a}, 1/500, Invitrogen) in blocking buffer containing 0.5% TX-100. Alexa 488-conjugated anti-mouse IgG and Alexa 568-conjugated anti-rabbit IgG were used as secondary antibodies (1/1000, Invitrogen). Fluorescent images were captured by confocal microscopy (FV500, Olympus) and the images were analyzed by Image J software (provided by NIH).

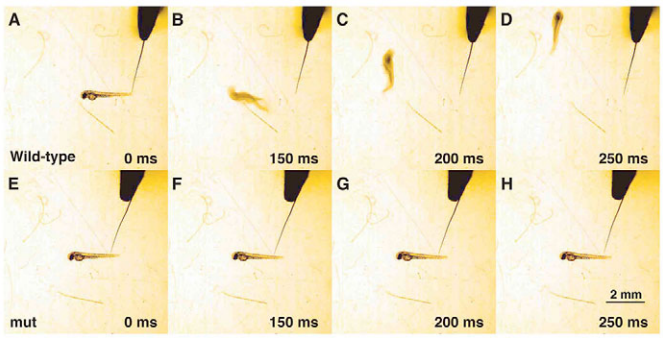

Fig. 1. *mi310* embryos do not respond to touch. (**A-D**) Mechanosensory stimulation induced a wild-type embryo [2 days post-fertilization (dpf)] to swim away rapidly. (**E-H**) A *mi310* embryo (2 dpf) did not respond to touch.

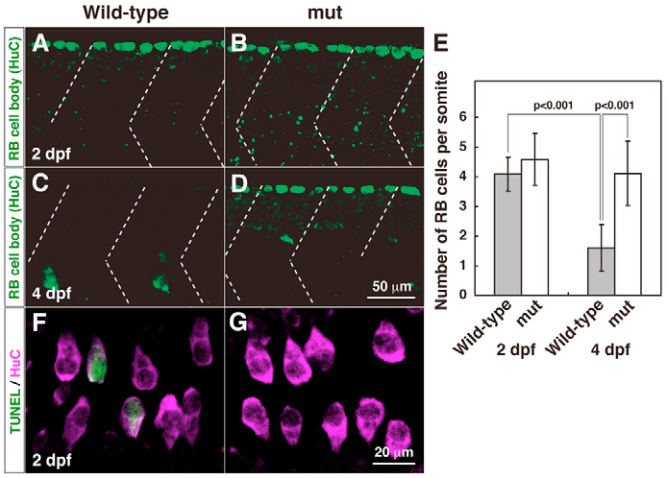

Fig. 2. Programmed cell death of RB neurons is diminished in *mi310* mutants. (**A**) In a lateral view of a wild-type embryo at 2 dpf, anti-HuC labeled large cell bodies of RB neurons (green). Dashed lines represent somite boundaries. (**B**) A mutant embryo displayed a comparable number of HuC-positive cells at 2 dpf. (**C**) In wild type, RB neurons were eliminated by 4 dpf. (**D**) HuC-positive RB cells were observed in mutant larva at 4 dpf. (**E**) The number of RB neurons is significantly reduced between 2 and 4 dpf in wild type but not in mutants. (**F**) In a dorsal view of a wild-type embryo, some HuC-positive neurons (magenta) were also positive for TUNEL (green) at 2 dpf. (**G**) HuC-TUNEL double-positive neurons were rarely observed in mutants.

RESULTS

mi310 mutants do not respond to tactile stimuli

A recessive mutation, *mi310*, was identified in an N-ethyl-N-nitrosourea mutagenesis screen. When wild-type embryos were touched with an eyelash at 2 days post-fertilization (dpf), they swam away from the stimuli (Fig. 1A-D; see Movie 1 in the supplementary material) (Saint-Amant and Drapeau, 1998). By contrast, *mi310* mutants did not respond to touch and remained motionless in the water (Fig. 1E-H; see Movie 2 in the supplementary material). To test whether the motor system is dysfunctional in mutants, we observed spontaneous swimming following bath application of NMDA, which can activate the locomotor network and induce swimming in lamprey and zebrafish (Di Prisco et al., 1997; Cui et al., 2004). Within 10 minutes of NMDA application, 55% (11/20) of wild-type embryos (see Movie 3 in the supplementary material) and 50% (10/20) of mutants (see Movie 4 in the supplementary material) showed spontaneous swimming with comparative latencies (wild-type: 280±151 seconds, n=11; mutants: 244±155 seconds, n=9). These behavioral analyses suggest that touch perception, rather than swimming capability, is affected in mutants at 2 dpf. The touch-insensitive phenotype in mutants was obvious even at 1 dpf; however, at this stage, 7.1% (3/42) of mutants rarely exhibited touch-evoked coilings, with the probability of once in 5-10 trials of tactile stimuli. Thus, we phenotypically identified and characterized the mutants at 2 dpf.

No obvious morphological defects were seen in mutant RB neurons, hindbrain neurons, motoneurons, neuromuscular junctions or muscles at 2 dpf (see Fig. S1 in the supplementary material). After 4 dpf, wild-type larvae swam spontaneously and fed on paramecia, whereas mutants remained immotile. Mutant larvae became thinner and died at ~7-10 dpf, probably owing to starvation because mutants without cardiac defects also died at the same period.

It has been reported that *macho* and five other *macho*-class mutants exhibit a touch-insensitive phenotype, which is likely to be comparable to *mi310* immobility (see Table S1 in the supplementary material) (Granato et al., 1996). However, we assume that *mi310* was not a new allele of either *macho* or other *macho*-class mutants because genetic mapping revealed that the chromosome carrying the *mi310* mutation (chromosome 6, discussed later in the paper) was distinct from those harboring *macho* or other *macho*-class mutations (see Discussion).

Programmed cell death of Rohon-Beard neurons is decreased in *mi310* mutants

The *macho* mutants display a reduction of RB cell death after 2 dpf (Svoboda et al., 2001), whereas the apoptosis of RB neurons has not been examined in other *macho*-class mutants. To assess whether the programmed cell death is also affected in *mi310* mutants, we counted the number of RB cells at 2 and 4 dpf. Although the monoclonal antibody zn12 has been typically used to label RB cell bodies and processes at 1-2 dpf, labeling with this antibody at later times post-fertilization shows labeling only in peripheral processes but not in the cell bodies of the RB neuron (Reyes et al., 2004), thus making it an inadequate marker in this case. To visualize long-lived RB neurons, we used anti-HuC, which labels RB cell bodies even after 2 dpf. The average number of RB cells in a somite at 2 dpf was comparable between wild-type (4.1±0.6, n=12; Fig. 2A,E) and mutants (4.6±0.9, n=12; Fig. 2B). By 4 dpf, however, the number of RB cells had decreased in wild-type (1.6±0.8, n=17; P<0.001, Student's t-test; Fig. 2C), whereas HuC-positive RB neurons remained relatively constant in mutants (4.1±1.1, n=19; Fig. 2D). To directly ascertain whether the RB cell death is decreased in mutants, we demonstrated anti-HuC immunolabeling with a terminal deoxynucleotidyl transferase-mediated dUTP nick-end-labeling (TUNEL) assay, which displays apoptic cells. In wild-type, a population of RB cells were colabeled by TUNEL at 2 dpf (Fig. 2F). By contrast, HuC and TUNEL double-positive RB cells were rarely found in mutants (Fig. 2G). These results indicate that the programmed cell death of RB neurons is diminished in *mi310* mutants, as in *macho* mutants, thereby raising the possibility that *mi310* mutants also have defects in generation of action potentials, which is required for programmed cell death of RB neurons.

Mutant RB neurons do not generate normal action potentials

To examine electrophysiological properties of RB neurons, we performed whole-cell patch-clamp recordings on semi-intact preparations of 2 dpf zebrafish embryos (see Fig. S2A in the supplementary material). We used a zCREST2-hsp70:GFP transgenic line, in which GFP is expressed by RB neurons and some interneurons (Uemura et al., 2005). Following sequential removal of skin, muscle and meninges, large GFP-positive RB cell bodies in the dorsal spinal cord were accessible to glass electrodes. After recording, the patched RB cell was morphologically confirmed by rhodamine diffusion (see Fig. S2B-E in the supplementary material). Resting membrane potential (wild-type: –69.1±6.5 mV, n=21; mutant: –69.5±6.2 mV, n=21), input resistance (wild-type: 2.0±0.9 GΩ, n=21; mutant: 2.1±1.6 GΩ, n=21) and membrane capacitance (wild-type: 3.2±0.9 pF, n=21; mutant: 3.1±0.6 pF, n=21) of RB neurons were comparable between wild-type and mutant embryos.

We examined generation of action potentials in RB cells at 2 dpf. In wild-type cells, typical action potentials were elicited by applying depolarizing currents (Fig. 3A), whereas no, or only partial, spikes were mostly observed in mutants (Fig. 3B). Indeed, all (100%, 17/17) of the wild-type RB neurons exhibited overshoots, whereas only 14.3% (3/21) of mutant RB neurons showed the active responses. Bath application of 0.5 μM TTX, a pharmacological blocker of voltage-gated sodium channels, completely eliminated the sharp spikes in wild type and partial spikes in mutants (Fig. 3C,D), showing that the action potentials were mediated by the TTX-sensitive voltage-gated sodium channels. To quantitatively compare action potentials, we calculated the maximum dV/dt, which represents the extent of sodium channel number. The maximum dV/dt in mutant traces (4.8±1.9 V/s, n=21) was significantly lowered compared with wild type (43.3±4.2 V/s, n=17; P<0.001, Student's t-test). These data indicate that mutant RB neurons fail to elicit normal action potentials and suggest that voltage-gated sodium channels are impaired in mutants.

Because the action potentials are produced by activation of voltage-gated sodium and potassium channels, we next demonstrated inward sodium currents in wild-type and mutant RB neurons. To isolate sodium currents, potassium components were eliminated by filling the intracellular patch solution with cesium chloride instead of potassium chloride. In wild-type RB cells, rapidly activating and inactivating inward currents were observed in response to stepwise depolarizations (Fig. 3E). These currents were completely blocked by 0.5 μM TTX (Fig. 3G), confirming that the inward currents are mediated by the voltage-gated sodium channels. By contrast, the amplitude of inward sodium currents was smaller in mutant RB neurons (Fig. 3F). The small currents in mutants were also TTX-sensitive (Fig. 3H). In the absence of TTX, some inward sodium currents were elicited after a short (~2.5 ms) delay, suggesting that the space clamps of voltage are poor in both wild-type and mutant RB cells. This suggestion is reasonable because RB neurons have long axons that preclude complete clamp of membrane potentials (Ribera and Nüsslein-Volhard, 1998). Thus, for quantitative comparison, we measured the maximum amplitude of sodium currents in each neuron. The maximum amplitude of sodium currents was significantly reduced in mutants (316±169 pA, n=21) compared with wild type (665±194 pA, n=17; P<0.001, Student's t-test). These data disclose that voltage-gated sodium channels are impaired in mutant RB neurons.

To assess whether the other membrane channels are affected in mutant RB cells, we measured outward potassium currents in wild-type and mutant RB neurons after blocking sodium channels with 0.5 μM TTX. Delayed and long-lasting potassium currents were elicited by step depolarizations (see Fig. S3A,B in the supplementary material). The potassium current density at 0 mV pulse was comparable between wild type (0.96±0.14 pA/μm^2, n=8) and mutants (1.30±0.18 pA/μm^2, n=10; P>0.3, Student's t-test; see Fig. S3C in the supplementary material), indicating that voltage-gated potassium channels are not affected in mutant RB neurons. These current- and voltage-clamp experiments clearly reveal that mutant RB neurons fail to generate action potentials owing to hypofunction of voltage-gated sodium channels. The loss of touch response in *mi310* mutants is attributable to the lack of firing in mutant RB cells.

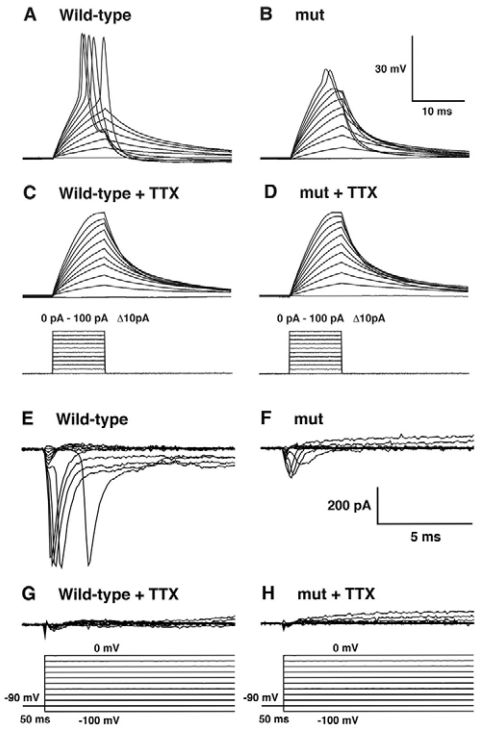

Fig. 3. Mutant RB neurons fail to generate normal action potentials owing to defective sodium currents. (**A**) Injection of step currents up to 100 pA elicited typically large action potentials in a wild-type RB neuron. (**B**) Current injection into a mutant RB cell failed to generate normal action potentials. (**C**) The spikes in wild-type RB neurons were eliminated by bath application of TTX, a sodium channel blocker. (**D**) The small, partial spikes in mutant RB neurons were also eliminated by TTX. (**E**) Inward sodium currents elicited by voltage steps from –100 mV to 0 mV were recorded in wild-type RB neurons. (**F**) Inward sodium currents in mutant RB neurons were observed but with smaller amplitude than those seen in wild-type neurons. (**G**) The inward sodium currents in wild type were blocked in the presence of TTX. (**H**) The sodium currents in mutant RB cells were also eliminated by TTX.

Cell surface expression of sodium channels is perturbed in mutant RB neurons

To see how voltage-gated sodium channels are defective in mutant RB neurons, the distribution of sodium channels was demonstrated by immunostaining. A sodium channel comprises a pore-forming α subunit (Nav) and an auxiliary β subunit (Scn1b) (Cantrell and Catterall, 2001; Isom et al., 1994). Zebrafish RB neurons are identifiable by their large, HuC-positive cell bodies in the dorsal

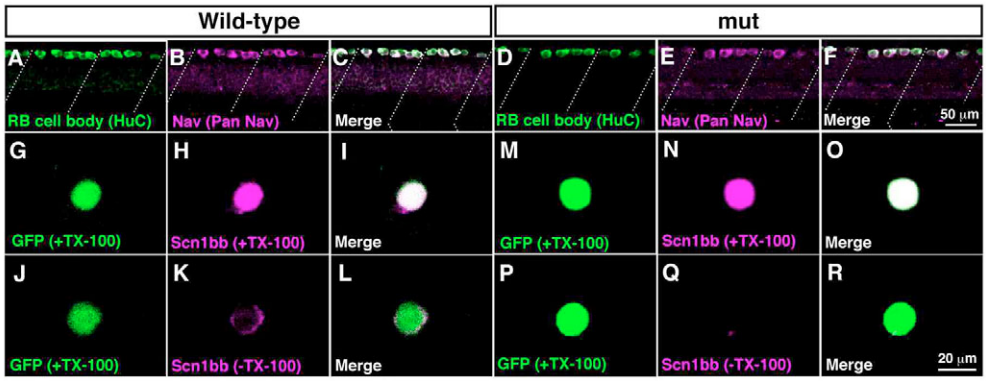

Fig. 4. Surface expression of sodium channels is impaired in mutant RB neurons. (**A-F**) Wholemount immunostaining showed Nav expression in wild-type and mutant RB neurons at 2 dpf. (A) Anti-HuC labeled cell bodies of wild-type RB neurons at the dorsal spinal cord. Dotted lines represent somite boundaries. (B) Immunostaining with anti-pan Nav displayed Nav expression in wild-type spinal cord. (C) A merged image showed that all HuC-positive RB cells expressed Nav in wild-type. (D) Labeling with anti-HuC showed RB neurons in mutant spinal cord. (E) Anti-pan Nav labeled dorsally located spinal neurons in mutants. (F) All of the HuC-positive mutant RB neurons expressed Nav. (**G-R**) Dissociated RB neurons (GFP-positive) from 2 dpf embryos were labeled with anti-Scn1bb, with or without TX-100, which permeabilizes the plasma membrane. Note that anti-Scn1bb reacts with the extracellular domain of Scn1bb. (G-I) Scn1bb staining in the permeable condition (+TX-100) demonstrated Scn1bb expression in a wild-type RB neuron. (J-L) Labeling of Scn1bb in the impermeable condition (–TX-100) displayed surface distribution of Scn1bb in a wild-type RB cell. (M-O) Scn1bb staining with TX-100 showed Scn1bb expression in a wild-type RB neuron. (P-R) In the absence of TX-100, the surface labeling of Scn1bb was missing in a mutant RB cell, suggesting that Scn1bb exists inside the mutant cell without expression at the surface.

spinal cord (Fig. 4A,D). Labeling with anti-pan Nav, which recognizes all types of sodium channel α subunits, showed that Nav were expressed by all RB cells in wild type (Fig. 4B,C) as well as in mutants (Fig. 4E,F), indicating that expression of sodium channels appears to be normal in mutant RB cells.

As our electrophysiological analyses reliably demonstrated the functional deficits of voltage-gated sodium channels, we next addressed whether sodium channels are expressed at the cell surface. On the one hand, the anti-pan Nav antibody binds to the intracellular loop of Nav (Vabnick et al., 1996), and thus is unavailable to label Nav protein distributed at the cell surface. On the other hand, anti-Scn1bb recognizes the extracellular domain, and thus might be suitable to label surface distribution of Scn1bb (Fein et al., 2007; Chopra et al., 2007; Fein et al., 2008). We tried labeling of surface Scn1bb in wholemount embryos; however, RB cells were not labeled in the absence of TX-100 in wild-type embryos owing to poor penetration (data not shown). We then dissociated RB neurons from wild-type and mutant embryos, both of which carry the zCREST2-hsp70:GFP transgene, initially labeled with anti-Scn1bb in the permeable (with TX-100) or the impermeable (without TX-100) condition and eventually stained with anti-GFP in the permeable condition. Labeling with anti-Scn1bb in the presence of TX-100 displayed Scn1bb expression in large, GFP-positive wild-type RB neurons (n=6; Fig. 4G-I), whereas Scn1bb distribution was observed only at the cell surface when labeled in the absence of TX-100 (n=4; Fig. 4J-L), corroborating the fact that this antibody acts on the extracellular domain. Mutant RB cells were also labeled with anti-Scn1bb when cells were permeabilized with TX-100 (n=5; Fig. 4M-O). However, Scn1bb was not stained or significantly reduced at the cell surface when immunolabeled without TX-100 (n=5; Fig. 4P-R). These results indicate that surface expression of sodium channels is perturbed in mutant RB cells and that hypofunction of sodium channels in *mi310* mutants is attributable to the lack of functional sodium channels at the plasma membrane.

mi310 encodes for Pigu, which comprises GPI transamidase

To identify the gene responsible for the *mi310* mutant phenotype, we meiotically mapped the mutation to a 160 kb region in chromosome 6 defined by two designed polymorphic markers (BX530017#2: 0.07 cM, 2 recombinations in 1527 mutants; CT030737#10: 0.07 cM, 2 recombinations in 1527 mutants; Fig. 5A). A gene encoding for phosphatidylinositol glycan anchor biosynthesis class U (Pigu), in which there was no recombination with a polymorphic marker (BX530017#7: <0.03 cM, 0 recombinations in 1527 mutants), was found in the crucial region. Pigu is one of five subunits of GPI transamidase that attaches glycosylphosphatidylinositol (GPI) to proteins containing GPI-anchoring C-terminal signal peptides (Hong et al., 2003). This anchoring reaction in the endoplasmic reticulum enables the GPI-anchored proteins to localize at the cell surface (Kinoshita et al., 2008). To assess whether *mi310* harbors a mutation in the *pigu* gene, zebrafish *pigu* cDNA was cloned and sequenced from wild-type and mutant embryos. Wild-type *pigu* encoded 435 amino acids that contained a signal peptide at the N-terminus and eight predicted membrane domains (GenBank #AB489197; Fig. 5B). In *mi310* mutants, Ile-86 was changed to Arg. This Ile residue in the first membrane domain was completely conserved among vertebrates.

The molecular identification of *mi310* was confirmed by mRNA rescue and antisense phenocopy. We injected wild-type or mutant (I86R) *pigu* mRNA into recently fertilized embryos of *mi310* heterozygous carriers. Approximately 27% (15/56) of the progeny injected with mutant *pigu* mRNA failed to display escape behavior at 2 dpf. By contrast, only 6% (3/47) of wild-type *pigu* mRNA-injected progeny was insensitive to touch. These results suggest that wild-type *pigu* mRNA rescued the normal touch response in mutants. We also injected mutant *pigu* mRNA into wild-type embryos and found no touch-insensitive phenotype, confirming that *pigu* mutation does not have dominant effects.

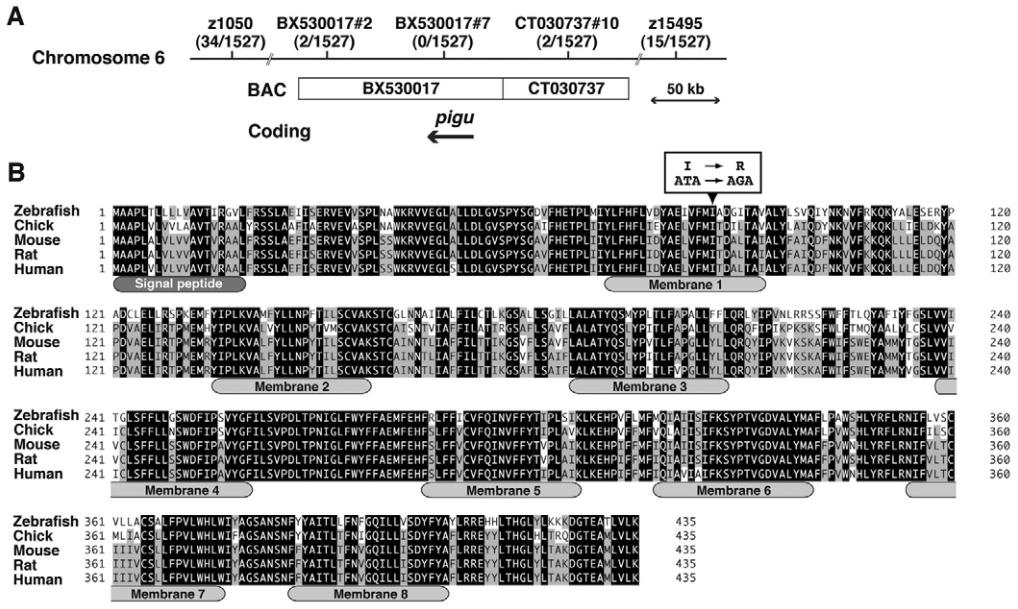

Fig. 5. *mi310* encodes for Pigu. (**A**) Meiotic mapping placed the *mi310* locus in a 160 kb region between two polymorphic markers, BX530017#2 and CT030737#10, in chromosome 6. No recombination was found with a polymorphic marker (BX530017#7) in the *pigu* gene. (**B**) Protein alignment of vertebrate Pigu. Shaded residues indicate conserved amino acids. Signal peptide and eight predicted membrane domains are indicated. Note that Ile-86, which was mutated in *mi310*, is completely conserved among vertebrates.

Furthermore, to directly demonstrate the behavioral restoration in homozygous mutants, we injected wild-type *pigu* mRNA into recently fertilized embryos of *mi310* heterozygous carriers, observed the individual touch responses and identified their genotype by direct sequencing of genomic PCR products. Among 31 homozygous mutants, 27 embryos (87%) exhibited normal tactile-evoked swimming following injection of wild-type mRNA, whereas only 4 embryos (13%) failed to respond to touch, corroborating that injection of wild-type mRNA successfully rescued the normal behavior in mutants. Next, to knockdown Pigu protein synthesis, antisense morpholino oligonucleotides (MO) were designed to block translation of *pigu* mRNA. The antisense *pigu* MO-injected wild-type embryos did not swim away after touch (91%, 80/88), whereas none of the control MO-injected embryos exhibited defective behavior (0%, 0/63). In addition, dissociated RB neurons from the *pigu* morphants demonstrated the absence of surface Scn1bb expression (Fig. 6G-I, *n*=3; Fig. 6J-L, *n*=3), whereas those from control morphants showed surface distribution of Scn1bb (Fig. 6A-C, *n*=3; Fig. 6D-F, *n*=3). The effects of mRNA rescue and antisense knockdown confirm that *mi310* encodes for Pigu.

To address whether the I86R mutation in Pigu abolishes the activity of GPI transamidase, we performed complementation tests using Pigu-deficient cultured cells, which had been generated by ethyl-methyl-sulfonate mutagenesis (Hong et al., 2003). We transiently transfected Pigu mutant Chinese hamster ovary (CHO) cells with expression vector carrying either human wild-type Pigu, the human I86R mutant, zebrafish wild-type Pigu or the zebrafish I86R mutant. Transamidase activity was estimated by surface expression of GPI-anchored proteins such as CD59 and DAF using flow cytometry. In the control vector transfection, neither CD59 nor DAF were labeled by fluorescent-conjugated antibodies because the cells lacked Pigu and thus failed to anchor CD59 and DAF at the plasma membrane (Fig. 7A). Overexpression of human PIGU restored the surface expression of both CD59 and DAF in the PIG-U-deficient cells. By contrast, transfection of human PIGU harboring the I86R mutation showed no such recovery. Similarly, overexpression of wild-type zebrafish Pigu, but not the I86R mutant, restored the surface distribution of GPI-anchored proteins. To verify whether wild-type and mutant Pigu protein were expressed in CHO cells, we performed immunoblots with anti-HSV, as each Pigu construct contains an HSV-tag at the C terminus (Fig. 7B). Both human and zebrafish wild-type Pigu proteins were intensely expressed in CHO cells, whereas the protein level of either the human or zebrafish I86R mutant was significantly low. These results, along with the rescue and knockdown experiments, indicate that the I86R mutation destabilizes the Pigu protein and diminishes the GPI transamidase activity that, in turn, affects the surface distribution of voltage-gated sodium channels, thereby abrogating the touch response

pigu is expressed ubiquitously

As *mi310* mutants have defects in RB neurons at 2 dpf, *pigu* should be expressed in RB cells. Indeed, in situ hybridization with an antisense probe showed that *pigu* mRNA was expressed in the whole embryo at 1 and 2 dpf (Fig. 8A-D), whereas no signal was observed by staining with a sense probe (Fig. 8K-N). These results are consistent with the fact that RB neurons are affected in mutants. Expression of *pigu* mRNA was also observed at the early cleavage stage (Fig. 8E-H,O-R), as well as sphere and segmentation stages (Fig. 8I,J,S,T), the former demonstrating that *pigu* is maternally expressed in zebrafish.

GPI transamidase is essential for the surface expression of sodium channels

To further ascertain whether GPI transamidase is necessary for the proper localization of sodium channels in RB neurons and for touch-elicited behavior, we demonstrated antisense knockdown of Gpi8, also known as Pigk (phosphatidylinositol glycan class K), a catalytic subunit of GPI transamidase (Benghezal et al., 1996; Ohishi et al., 2000). Similar to the *pigu* knockdown, *gpi8* MO-injected embryos did not display escape behavior after touch (93%, 38/41). Furthermore, immunolabeling confirmed that surface expression of Scn1bb was decreased in RB neurons dissociated from *gpi8* morphants (Fig. 6M-O, *n*=5; Fig. 6P-R, *n*=5). These behavioral defects and misdistribution of Scn1bb in *gpi8* morphants are indistinguishable from those in *mi310* mutants and *pigu* morphants,

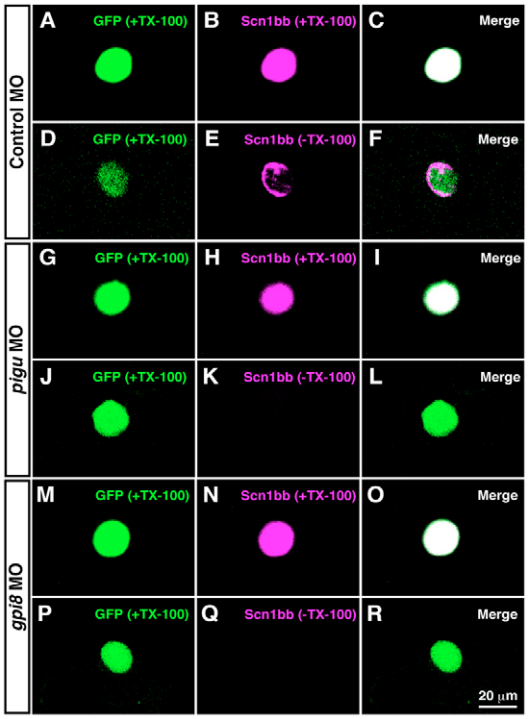

Fig. 6. Surface distribution of Scn1bb in RB neurons is diminished by knocking down GPI transamidase subunits. Dissociated RB neurons (GFP-positive) from 2 dpf embryos were labeled with anti-Scn1bb in the permeable (+TX-100) or impermeable (–TX-100) condition. (**A-F**) In control morpholino (MO)-injection, anti-Scn1bb labeled a whole RB cell in the presence of TX-100 (A-C), whereas it labeled the circumference of an RB cell in the absence of TX-100 (D-F). (**G-I**) Labeling with anti-Scn1bb with TX-100 displayed Scn1bb expression in an RB cell dissociated from a *pigu* morphant. (**J-L**) Scn1bb staining without TX-100 represented the impairment of Scn1bb surface distribution in a *pigu* morphant RB neuron. (**M-O**) Scn1bb labeling with TX-100 showed Scn1bb expression in a *gpi8* morphant RB cell. (**P-R**) The surface expression of Scn1bb was not seen in an RB cell dissociated from a *gpi8* morphant.

recapitulating the notion that GPI transamidase activity is responsible for the surface expression of sodium channels and, consequently, for the normal touch response.

DISCUSSION

In this study, we studied zebrafish *pigu* mutants, which do not respond to mechanosensory stimulation. A mis-sense mutation in *pigu* destabilized the Pigu protein and disrupted GPI transamidase activity. Surface expression of sodium channels in the sensory RB neurons was diminished in mutants, thereby compromising the generation of action potentials. Taken together, GPI transamidase is essential for the surface expression of voltage-gated sodium channels and thus for touch-evoked escape behavior.

RB neurons are affected in *mi310* mutants

Zebrafish *mi310* mutants did not show touch-evoked swimming at 2 dpf. However, bath application of NMDA, which activates the locomotor network within the CNS, induced spontaneous swimming in mutants as it did in wild-type embryos, suggesting that the mechanosensory RB neurons, rather than the downstream motor circuits, are primarily affected in mutants. In accordance with this expectation, swirling of the embryo container that

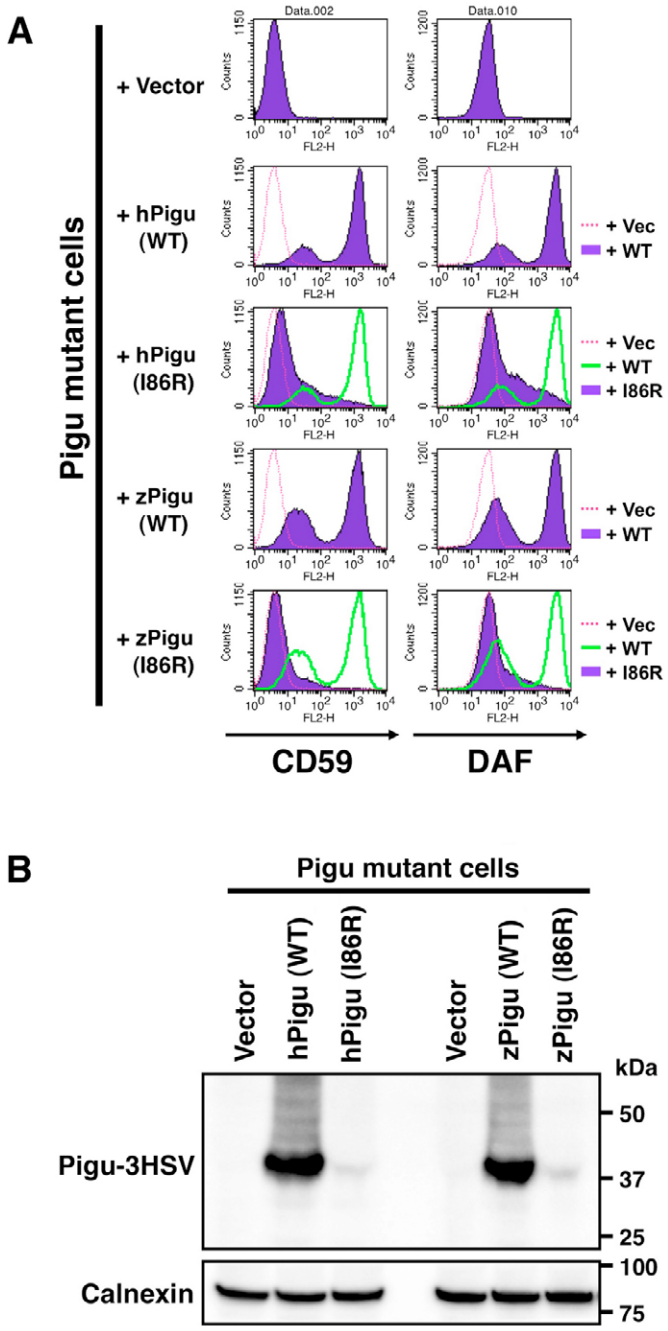

Fig. 7. Wild-type Pigu restores the surface expression of GPI-anchored proteins in Pigu-deficient CHO cells. (**A**) Control or Pigu expression vectors were transfected into Pigu mutant CHO cells and the surface expressions of GPI-anchored proteins (CD59 and DAF) were estimated by flow cytometry. Surface expressions of CD59 and DAF were lower in vector-transfected Pigu mutant cells. Following transfection of human wild-type PIGU or zebrafish wild-type Pigu, surface expressions of CD59 and DAF were increased, showing that GPI transamidase activity was restored by expression of wild-type Pigu. Recovery of surface distribution of GPI-anchored proteins was not seen when transfected with human mutant (I86R) PIGU or zebrafish mutant (I86R) Pigu constructs. (**B**) The I86R mutation in Pigu destabilized the protein. Whole cell extracts from each pool of the transfected CHO cells were probed with anti-HSV to examine Pigu protein levels. Compared with human and zebrafish wild-type Pigu expressions, the protein levels of human PIGU (I86R) and zebrafish PIGU (I86R) were significantly lower. Calnexin is used as a loading control.

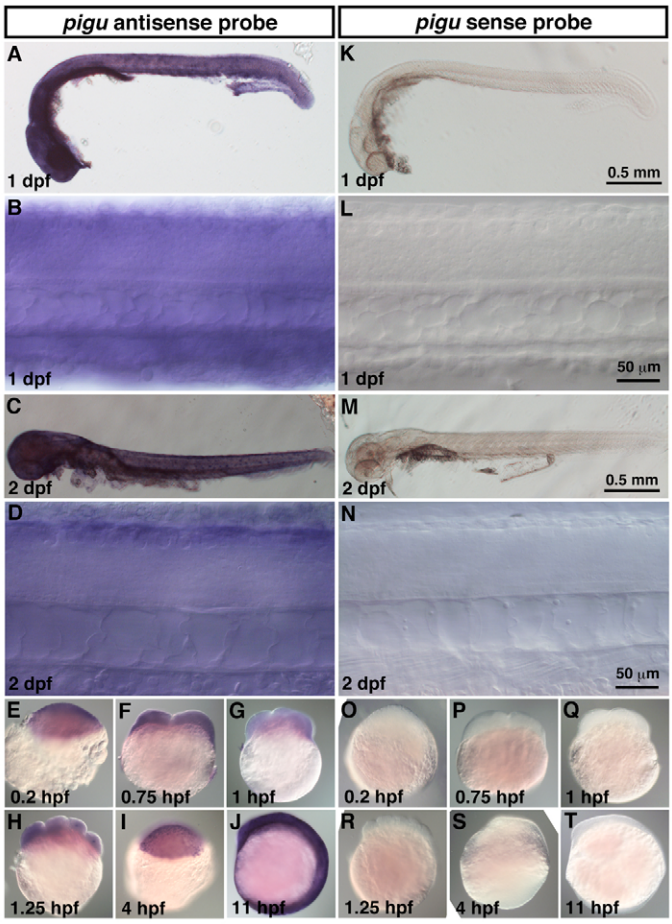

Fig. 8. *pigu* is expressed ubiquitously by whole embryos. In situ hybridization with *pigu* antisense (**A-J**) or sense probes (**K-T**). Wholemounts and DIC images at the spinal cord showed that *pigu* is expressed by whole zebrafish embryos at 1 dpf (A,B) and 2 dpf (C,D). Expression of *pigu* mRNA was also observed at 0.2 hpf (1-cell stage; E), 0.75 hpf (2-cell stage; F), 1 hpf (4-cell stage; G), 1.25 hpf (8-cell stage; H), 4 hpf (sphere stage; I) and 11 hpf (early segmentation stage; J). Staining with sense probe displayed no *pigu* expression at any stages (K-T).

activates lateral line neurons, which detect water flow (Ma and Raible, 2009), also triggered normal swimming in mutants (data not shown). These NMDA- and swirl-mediated swimming behaviors support the notion that post-sensory motor function is not affected in mutants. Furthermore, the lack of cell surface distribution of Scn1bb and the subsequent reduction of TTX-sensitive sodium currents in mutant RB neurons accounts for the failure of mutant RB neurons to fire. These facts strongly suggest that dysfunction of RB neurons is the primary cause of the defective touch response in mutants.

It has been suggested that electrical activity mediated by voltage-gated sodium channels is necessary for the programmed cell death of RB neurons because the RB cell death is reduced in Nav1.6 morphants (Svoboda et al., 2001). The fact that the apoptosis of RB cells is diminished in *mi310* mutants corroborates the hypothesis. Although neuronal activity generally promotes cell survival (Cohen and Greenberg, 2008), activity-dependent cell death is not unusual during embryogenesis. For instance, the blocking of synaptic inputs reduces normally occurring apoptosis of motoneurons in chick development (Pittman and Oppenheim, 1979). However, little is known about the mechanism of how zebrafish RB neurons die in an activity-dependent manner (Kanungo et al., 2009). As the apoptosis of RB cells is also compromised by overexpression of cyclin-dependent kinase 5 (Cdk5) (Kanungo et al., 2006), electrical activity mediated by voltage-gated sodium channels might negatively regulate Cdk5 activity to promote the RB cell death.

Although, in *mi310* mutants, biogenesis of GPI-anchored proteins might be affected not only in RB neurons but also in of all the other cells, the mutant phenotype was specifically linked to the RB cells at 2 dpf. In fact, NMDA-induced swimming was normally observed in mutants, suggesting that motoneurons appear to be normal in mutants. We tried surface labeling of Scn1bb in motoneurons dissociated from hb9:Venus transgenic fish; however, anti-Scn1bb did not label either the surface or inside of wild-type motoneurons, probably because another β subunit, but not Scn1bb, is expressed in motoneurons. Intriguingly, *mi310* mutant embryos and larvae do not display apparent morphological defects by 5 dpf. One would predict that maternal supply of *pigu* mRNA cancels the developmental perturbation. However, it is not probable because injection of *pigu* antisense MO, which eliminates both maternal and zygotic synthesis of Pigu protein, into homozygous mutants did not cause any developmental malformations (data not shown). Thus, it appears that RB neurons are sensitive to the deficiency of GPI-anchored proteins.

mi310 gene and other touch-insensitive mutants

We identified an I86R mis-sense mutation in the Pigu of *mi310* mutants. This mutation in the predicted first membrane domain probably affected the hydrophobicity of the membrane domain, which, in turn, caused a reduction in the protein stability. It has been demonstrated that abnormal proteins resulting from impaired modification or misfolding in the endoplasmic reticulum (ER) are actively degraded by the ER-associated degradation (ERAD) system (Vembar and Brodsky, 2008). Thus, the degradation of mutant Pigu protein in the ER might also be accelerated in this manner.

The large-scale Tübingen mutagenesis screen isolated six mutants [*macho*, *alligator*, *steifftier*, *brudas* (*crocodile*), *schlaffi* and *fakir*] that display reduced or no response to tactile stimuli (Granato et al., 1996). Among them, four mutants (*macho*, *alligator*, *steifftier* and *brudas*) showed a hypofunction of voltage-gated sodium channels in RB neurons, whereas the excitability of RB cells was normal in *schlaffi* (Ribera and Nüsslein-Volhard, 1998). Subsequent analyses revealed that *macho* exhibited a reduction in RB cell death (Svoboda et al., 2001); however, the other *macho*-class mutants have not been examined to determine whether RB neurons undergo apoptosis. In this study, we found that *mi310* mutants display several phenotypes indistinguishable from those of *macho*. First, both *macho* and *mi310* mutants failed to respond to mechanosensory stimulation, but both displayed spontaneous swimming (Granato et al., 1996; Ribera and Nüsslein-Volhard, 1998). Second, the programmed cell death of RB neurons was impaired in both mutants. Finally, RB cells failed to elicit action potentials, owing to the defective voltage-gated sodium channels in both mutants. In spite of these identical phenotypes, *mi310* mutation is not a new allele of *macho* or other *macho*-class mutations because the *mi310* gene (*pigu*) was found to be located in chromosome 6, whereas *macho* and other *macho*-class mutations were respectively mapped in distinctly different chromosomes (see Table S1 in the supplementary material). This study demonstrates the first molecular identification of a touch-insensitive mutation that might provide an insight toward the understanding of *macho* and other *macho*-class mutants. Indeed, antisense knockdown of Gpi8 (Pigk), another subunit of GPI transamidase (Benghezal et al., 1996;

Ohishi et al., 2000), phenocopied *mi310* mutants, and as both the *gpi8* gene and *macho* mutation are located in chromosome 2, *gpi8* is probably a good candidate for the *macho* gene.

What is the target of GPI transamidase?

We found that GPI transamidase is essential for physiologically relevant surface expression of voltage-gated sodium channels in RB neurons. However, it remains unclear how GPI transamidase acts on the sodium channels. Neither the α nor β subunit of the voltage-gated sodium channel is a GPI-anchored protein (Cantrell and Catterall, 2001; Isom et al., 1994), raising the possibility that an unidentified GPI-anchored protein mediates cell surface expression of sodium channels. In vertebrates, defective surface expression of transmembrane proteins has not been linked to a lack of GPI-anchored proteins; however, a mutation in yeast *gaa1*, which encodes one of the five subunits of GPI transamidase, impairs expression of Tat2p, encoding tryptophan permease, at the plasma membrane (Hamburger et al., 1995; Okamoto et al., 2006). In addition, a yeast mutation in *gwt1* (PIGW in mammals), which is required for inositol acylaton in the GPI biosynthetic pathway, also affects Tat2p expression at the cell surface (Umemura et al., 2003; Okamoto et al., 2006). These facts suggest a possibility that biogenesis of GPI-anchored proteins is necessary for the surface expression of certain membrane proteins such as Tat2p in yeast and sodium channels in zebrafish.

It has been reported that mouse Scn1b interacts with contactin 1, a GPI-anchored protein that belongs to the contactin subgroup of the immunoglobulin superfamily (Falk et al., 2002; Katidou et al., 2008) and enhances the surface expression of sodium channels in cultured cells (Kazarinova-Noyes et al., 2001; McEwen et al., 2004; McEwen and Isom, 2004). These in vitro data suggest that contactin 1 is the most probable target of GPI transamidase to promote sodium channel expression at the RB cell surface. Owing to the suspected duplication of the whole genome, zebrafish have two paralogs of Contactin 1, Contactin 1a and Contactin 1b, the former expressed in RB neurons, and the latter in the retina and lens but not RB cells (Gimnopoulos et al., 2002; Haenisch et al., 2005). However, antisense knockdown of Contactin 1a did not perturb the touch-evoked swimming (data not shown). In addition, surface distribution of voltage-gated sodium channels was not perturbed in contactin 1-deficient mice, whereas the mutant mice displayed mislocalization of voltage-gated potassium channels (Berglund et al., 1999; Boyle et al., 2001), indicating that contactin 1 is not necessary for the proper expression of sodium channels in developing mice. Therefore, it appears that Contactin 1 is not the GPI-anchored protein that mediates surface expression of sodium channels in vivo. In zebrafish, we also examined antisense knockdown of either Contactin 2 (Tag1) (Warren et al., 1999), Contactin 4a, Contactin 4b or Contactin 5, alone or in combination of two or three Contactin genes, but none of the morphants displayed touch-insensitive phenotype (data not shown). Although we could not find the target of GPI transamidase in this study, further analyses will identify the GPI-anchored protein, which might be involved in the cell surface expression of voltage-gated sodium channels.

Acknowledgements

We thank Drs J. Y. Kuwada (University of Michigan), S. E. Low (Université de Montréal), S. M. Sprague (University of Michigan), W. W. Cui (University of California, San Francisco), W. Zhou (University of Michigan) and R.I. Hume (University of Michigan) for materials, technical support, helpful advice and encouragement. We also thank Drs H. Okamoto (RIKEN), L. Isom (University of Michigan), and S. Takagi (Nagoya University) and Y. Matsutani (Nagoya University) for providing zCREST2-hsp70:GFP transgenic zebrafish, anti-zScn1bb polyclonal antibody, insightful advice and daily care of zebrafish, respectively. The transgenic line was distributed through the National BioResource Project (Zebrafish). This work was supported by a Grant-in-Aid for Scientific Research on Priority Areas 'System Genomics', a Grant-in-Aid for Young Scientists (A) from the Ministry of Education, Culture, Sports, Science and Technology of Japan, and a Career Development Award of the Human Frontier Science Program awarded to H.H.; a grant from the National Science and Engineering Research Council of Canada, a Canadian Institutes of Health Research operating grant and a chercheur boursier award and the GRSNC from the Fond de Recherche en Santé du Québec awarded to L.S.-A.; and a Grant-in-Aid for Scientific Research on Priority Areas 'Elucidation of neural network function in the brain' awarded to Y.O.

Competing interests statement

The authors declare no competing financial interests.

Supplementary material

Supplementary material for this article is available at
http://dev.biologists.org/lookup/suppl/doi:10.1242/dev.047464/-/DC1

References

Andersen, S. S. L. (2002). Preparation of dissociated zebrafish spinal neuron cultures. *Methods Cell Sci.* **23**, 205-209.
Bahary, N., Davidson, A., Ransom, D., Shepard, J., Stern, H., Trede, N., Zhou, Y., Barut, B. and Zon, L. I. (2004). The Zon laboratory guide to positional cloning in zebrafish. *Methods Cell Biol.* **77**, 305-329.
Benghezal, M., Benachour, A., Rusconi, S., Aebi, M. and Conzelmann, A. (1996). Yeast Gpi8p is essential for GPI anchor attachment onto proteins. *EMBO J.* **15**, 6575-6583.
Berglund, E. O., Murai, K. K., Fredette, B., Sekerková, G., Marturano, B., Weber, L., Mugnaini, E. and Ranscht, B. (1999). Ataxia and abnormal cerebellar microorganization in mice with ablated contactin gene expression. *Neuron* **24**, 739-750.
Bernhardt, R. R., Chitnis, A. B., Lindamer, L. and Kuwada, J. Y. (1990). Identification of spinal neurons in the embryonic and larval zebrafish. *J. Comp. Neurol.* **302**, 603-616.
Boyle, M. E. T., Berglund, E. O., Murai, K. K., Weber, L., Peles, E. and Ranscht, B. (2001). Contactin orchestrates assembly of the septate-like junctions at the paranode in myelinated peripheral nerve. *Neuron* **30**, 385-397.
Cantrell, A. R. and Catterall, W. A. (2001). Neuromodulation of Na^+ channels: an unexpected form of cellular plasticity. *Nat. Rev. Neurosci.* **2**, 397-407.
Chopra, S. S., Watanabe, H., Zhong, T. P. and Roden, D. M. (2007). Molecular cloning and analysis of zebrafish voltage-gated sodium channel beta subunit genes: implications for the evolution of electrical signaling in vertebrates. *BMC Evol. Biol.* **7**, 113.
Cohen, S. and Greenberg, M. E. (2008). Communication between the synapse and the nucleus in neuronal development, plasticity, and disease. *Annu. Rev. Cell Dev. Biol.* **24**, 183-209.
Cole, L. K. and Ross, L. S. (2001). Apoptosis in the developing zebrafish embryo. *Dev. Biol.* **240**, 123-142.
Cui, W. W., Saint-Amant, L. and Kuwada, J. Y. (2004). *shocked* gene is required for the function of a premotor network in the zebrafish CNS. *J. Neurophysiol.* **92**, 2898-2908.
Di Prisco, G. V., Pearlstein, E., Robitaille, R. and Dubuc, R. (1997). Role of sensory-evoked NMDA plateau potentials in the initiation of locomotion. *Science* **278**, 1122-1125.
Falk, J., Bonnon, C., Girault, J. A. and Faivre-Sarrailh, C. (2002). F3/contactin, a neuronal cell adhesion molecule implicated in axogenesis and myelination. *Biol. Cell* **94**, 327-334.
Fein, A. J., Meadows, L. S., Chen, C., Slat, E. A. and Isom, L. L. (2007). Cloning and expression of a zebrafish *SCN1B* orthologs and identification of a species-specific splice variant. *BMC Genomics* **8**, 226.
Fein, A. J., Wright, M. A., Slat, E. A., Ribera, A. B. and Isom, L. L. (2008). *scn1bb*, a zebrafish ortholog of *SCN1B* expressed in excitable and nonexcitable cells, affects motor neuron axon morphology and touch sensitivity. *J. Neurosci.* **28**, 12510-12522.
Flanagan-Steet, H., Fox, M. A., Meyer, D. and Sanes, J. R. (2005). Neuromuscular synapses can form in vivo by incorporation of initially aneural postsynaptic specializations. *Development* **132**, 4471-4481.
Gates, M. A., Kim, L., Egan, E. S., Cardozo, T., Sirotkin, H. I., Dougan, S. T., Lashkari, D., Abagyan, R., Schier, A. F. and Talbot, W. S. (1999). A genetic linkage map for zebrafish: comparative analysis and localization of genes and expressed sequences. *Genome Res.* **9**, 334-347.
Gimnopoulos, D., Becker, C. G., Ostendorff, H. P., Bach, I., Schachner, M. and Becker, T. (2002). Expression of the zebrafish recognition molecule F3/F11/contactin in a subset of differentiating neurons is regulated by cofactors associated with LIM domains. *Mech. Dev.* **119S**, S135-S141.
Granato, M., van Eeden, F. J. M., Schach, U., Trowe, T., Brand, M., Furutani-Seiki, M., Haffter, P., Hammerschmidt, M., Heisenberg, C. P., Jiang, Y. J. et

al. (1996). Genes controlling and mediating locomotion behavior of the zebrafish embryo and larva. *Development* **123**, 399-413.
Haenisch, C., Diekmann, H., Klinger, M., Gennarini, G., Kuwada, J. Y. and Stuermer, C. A. O. (2005). The neuronal growth and regeneration associated Cntn1 (F3/F11/Contactin) gene is duplicated in fish: expression during development and retinal axon regeneration. *Mol. Cell. Neurosci.* **28**, 361-374.
Hamburger, D., Egerton, M. and Riezman, H. (1995). Yeast Gaa1p is required for attachment of a completed GPI anchor onto proteins. *J. Cell Biol.* **129**, 629-639.
Hirata, H., Saint-Amant, L., Waterbury, J., Cui, W. W., Zhou, W., Li, Q., Goldman, D., Granato, M. and Kuwada, J. Y. (2004). *accordion*, a zebrafish behavioral mutant, has a muscle relaxation defect due to a mutation in the ATPase Ca^{2+} pump SERCA1. *Development* **131**, 5457-5468.
Hirata, H., Saint-Amant, L., Downes, G. B., Cui, W. W., Zhou, W., Granato, M. and Kuwada, J. Y. (2005). Zebrafish *bandoneon* mutants display behavioral defects due to a mutation in the glycine receptor β-subunit. *Proc. Natl. Acad. Sci. USA* **102**, 8345-8350.
Hirata, H., Watanabe, T., Hatakeyama, J., Sprague, S. M., Saint-Amant, L., Nagashima, A., Cui, W. W., Zhou, W. and Kuwada, J. Y. (2007). Zebrafish *relatively relaxed* mutants have a ryanodine receptor defect, show slow swimming and provide a model of multi-minicire disease. *Development* **134**, 2771-2781.
Hong, Y., Ohishi, K., Kang, J. Y., Tanaka, S., Inoue, N., Nishimura, J., Maeda, Y. and Kinoshita, T. (2003). Human PIG-U and yeast Cdc91p are the fifth subunit of GPI transamidase that attaches GPI-anchors to proteins. *Mol. Biol. Cell* **14**, 1780-1789.
Isom, L. L., de Jongh, K. S. and Catterall, W. A. (1994). Auxiliary subunits of voltage-gated ion channels. *Neuron* **12**, 1183-1194.
Kanungo, J., Li, B. S., Zheng, Y. and Pant, H. C. (2006). Cyclin-dependent kinase 5 influences Rohon-Beard Neuron survival in zebrafish. *J. Neurochem.* **99**, 251-259.
Kanungo, J., Zheng, Y. L., Mishra, B. and Pant, H. C. (2009). Zebrafish Rohon-Beard neuron development: Cdk5 in the midst. *Neurochem. Res.* **34**, 1129-1137.
Katidou, M., Vidaki, M., Strigini, M. and Karagogeos, D. (2008). The immunoglobulin superfamily of neuronal cell adhesion molecules: Lessons from animal models and correlation with human disease. *Biotechnol. J.* **3**, 1564-1580.
Kawakami, K., Shima, A. and Kawakami, N. (2000). Identification of a functional transposase of the *Tol2* element, an *Ac*-like element from the Japanese medaka fish, and its transposition in the zebrafish germ lineage. *Proc. Natl. Acad. Sci. USA* **97**, 11403-11408.
Kazarinova-Noyes, K., Malhotra, J. D., McEwen, D. P., Mattei, L. N., Berglund, E. O., Ranscht, B., Levinson, S. R., Schachner, M., Shrager, P., Isom, L. L. et al. (2001). Contactin associates with Na^+ channels and increases their functional expression. *J. Neurosci.* **21**, 7517-7525.
Kinoshita, T., Fujita, M. and Maeda, Y. (2008). Biosynthesis, remodeling and functions of mammalian GPI-anchored proteins: recent progress. *J. Biochem.* **144**, 287-294.
Ma, E. Y. and Raible, D. W. (2009). Signaling pathways regulating zebrafish lateral line development. *Curr. Biol.* **19**, R381-R386.
McEwen, D. P. and Isom, L. L. (2004). Heterophilic interactions of sodium channel β1 subunits with axonal and glial cell adhesion molecules. *J. Biol. Chem.* **279**, 52744-52752.
McEwen, D. P., Meadows, L. S., Chen, C., Thyagarajan, V. and Isom, L. L. (2004). Sodium channel β1 subunit-mediated modulation of $Na_v1.2$ currents and cell surface density is dependent on interactions with contactin and ankyrin. *J. Biol. Chem.* **279**, 16044-16049.
Metcalfe, W. K., Myers, P. Z., Trevarrow, B., Bass, M. B. and Kimmel, C. B. (1990). Primary neurons that express the L2/HNK-1 carbohydrate during early development in the zebrafish. *Development* **110**, 491-504.
Nagai, T., Ibata, K., Park, E. S., Kubota, M., Mikoshiba, K. and Miyawaki, A. (2002). A variant of yellow fluorescent protein with fast and efficient maturation for cell-biological applications. *Nat. Biotechnol.* **20**, 87-90.
Nasevicius, A. and Ekker, S. C. (2000). Effective targeted gene 'knockdown' in zebrafish. *Nat. Genet.* **26**, 216-220.
Nüsslein-Volhard, C. and Dahm, R. (2002). *Zebrafish: A Practical Approach*. New York: Oxford University Press.
Ohishi, K., Inoue, N., Maeda, Y., Takeda, J., Riezman, H. and Kinoshita, T. (2000). Gaa1p and gpi8p are components of a glycosylphosphatidylinositol (GPI) transamidase that mediates attachment of GPI to proteins. *Mol. Biol. Cell* **11**, 1523-1533.
Okamoto, M., Yoko-o, T., Umemura, M., Nakayama, K. and Jigami, Y. (2006). Glycosylphosphatidylinositol-anchored proteins are required for the transport of detergent-resistant microdomain-associated membrane proteins Tat2p and Fur4p. *J. Biol. Chem.* **281**, 4013-4023.
Pineda, R. H., Heiser, R. A. and Ribera, A. B. (2005). Developmental, molecular, and genetic dissection of I_{Na} in vivo in embryonic zebrafish sensory neurons. *J. Neurophysiol.* **93**, 3582-3593.
Pineda, R. H., Svoboda, K. R., Wright, M. A., Taylor, A. D., Novak, A. E., Gamse, J. T., Eisen, J. S. and Ribera, A. B. (2006). Knockdown of $Na_v1.6a$ Na^+ channels affects zebrafish motoneuron development. *Development* **133**, 3827-3836.
Pittman, R. and Oppenheim, R. W. (1979). Cell death of motoneurons in the chick embryo spinal cord. IV. Evidence that a functional neuromuscular interactions is involved in the regulation of naturally occurring cell death and the stabilization of synapses. *J. Comp. Neurol.* **187**, 425-446.
Reyes, R., Haendel, M., Grant, D., Melancon, E. and Eisen, J. S. (2004). Slow degeneration of zebrafish Rohon-Beard neurons during programmed cell death. *Dev. Dyn.* **229**, 30-41.
Ribera, A. B. and Nüsslein-Volhard, C. (1998). Zebrafish touch-insensitive mutants reveal an essential role for the developmental regulation of sodium current. *J. Neurosci.* **18**, 9181-9191.
Roberts, A. (2000). Early functional organization of spinal neurons in developing lower vertebrates. *Brain Res. Bull.* **53**, 585-593.
Saint-Amant, L. and Drapeau, P. (1998). Time course of the development of motor behaviors in the zebrafish embryo. *J. Neurobiol.* **37**, 622-632.
Shimoda, N., Knapik, E. W., Ziniti, J., Sim, C., Yamada, E., Kaplan, S., Jackson, D., de Sauvage, F., Jacob, H. and Fishman, M. C. (1999). Zebrafish genetic map with 2000 microsatellite markers. *Genomics* **58**, 219-232.
Sidi, S., Sanda, T., Kennedy, R. D., Hagen, A. T., Jette, C. A., Hoffmans, R., Pascual, J., Imamura, S., Kishi, S., Amatruda, J. F. et al. (2008). Chk1 suppresses a caspase-2 apoptic response to DNA damage that bypasses p53, Bcl2, and Caspase-3. *Cell* **133**, 864-877.
Svoboda, K. R., Linares, A. E. and Ribera, A. B. (2001). Activity regulates programmed cell death of zebrafish Rohon-Beard neurons. *Development* **128**, 3511-3520.
Uemura, O., Okada, Y., Ando, H., Guedj, M., Higashijima, S., Shimazaki, T., Chino, N., Okano, H. and Okamoto, H. (2005). Comparative functional genomics revealed conservation and diversification of three enhancers of the *isl1* gene for motor and sensory neuron-specific expression. *Dev. Biol.* **278**, 587-606.
Umemura, M., Okamoto, M., Nakayama, K., Sagane, K., Tsukahara, K., Hata, K. and Jigami, Y. (2003). *GWT1* gene is required for inositol acylation of glycosylphosphatidylinositol anchors in yeast. *J. Biol. Chem.* **278**, 23639-23647.
Vabnick, I., Novakovi, S. D., Levinson, S. R., Schachner, M. and Shrager, P. (1996). The clustering of axon sodium channels during development of the peripheral nervous system. *J. Neurosci.* **16**, 4914-4922.
Vembar, S. S. and Brodsky, J. L. (2008). One step at a time: endoplasmic reticulum-associated degradation. *Nat. Rev. Mol. Cell Biol.* **9**, 944-957.
Warren, J. T., Jr, Chandrasekhar, A., Kanki, J. P., Rangarajan, R., Furley, A. J. and Kuwada, J. Y. (1999). Molecular cloning and developmental exopression of a zebrafish axonal glycoprotein similar to TAG-1. *Mech. Dev.* **80**, 197-201.
Westerfield, M. (2007). *The zebrafish book. A guide for the laboratory use of zebrafish (Danio rerio)*, 5th edn. Eugene: University of Oregon Press.
Williams, J. A., Barrios, A., Gatchalian, C., Rubin, L., Wilson, S. W. and Holder, N. (2000). Programmed cell death in zebrafish Rohon Beard neurons is influenced by TrkC1/NT-3 signaling. *Dev. Biol.* **226**, 220-230.

Table S1. *mi310* is a novel touch-insensitive mutation

	Chromosome	Touch-insensitive	Reduction of Na currents in RB neurons	Reduction of programmed RB cell death	References
mi310	6	Yes	Yes	Yes	This study
macho	2	Yes	Yes	Yes	Granato et al. (1996) Ribera and Nüsslein-Volhard (1998) Svoboda et al., (2001) Gnuegge et al., (2001) Pineda et al. (2005)
alligator	21	Yes	Yes	N/A	Granato et al. (1996) Ribera and Nüsslein-Volhard (1998) Geisler et al. (2007)
steifftier	24	Yes	Yes	N/A	Granato et al. (1996) Ribera and Nüsslein-Volhard (1998) Geisler et al. (2007)
brudas (*crocodile*)	3	Yes	Yes	N/A	Granato et al. (1996) Ribera and Nüsslein-Volhard (1998) Doerre and Malicki (2002)
schlaffi	7	Yes	No	N/A	Granato et al. (1996) Ribera and Nüsslein-Volhard (1998) Geisler et al. (2007)
fakir	11	Yes	N/A	N/A	Granato et al. (1996) Geisler et al. (2007)

Doerre, G. and Malicki, J. (2002). Genetic analysis of photoreceptor cell development in the zebrafish retina. *Mech. Dev.* **110**, 125-138.
Geisler, R., Rauch, G. J., Geiger-Rudolph, S., Albrecht, A., van Bebber, F., Berger, A., Busch-Nentwich, E., Dahm, R., Dekens, M. P., Dooley, C. et al. (2007). Large-scale mapping of mutations affecting zebrafish development. *BMC Genomics* **8**, 11.
Gnuegge, L., Schmid, S. and Neuhauss, S. C. (2001). Analysis of the activity-deprived zebrafish mutant *macho* reveals an essential requirement of neuronal activity for the development of a fine-grained visuotopic map. *J. Neurosci.* **21**, 3542-3548.